

Factors Influencing the Disturbed Flow Patterns Downstream of Curved Atherosclerotic Arteries

Biyue Liu*

*Department of Mathematics, Monmouth University, West Long Branch, NJ 07764,
USA.*

Received 28 June, 2007; Accepted (in revised version) 13 November, 2007

Abstract. Pulsatile blood flows in curved atherosclerotic arteries are studied by computer simulations. Computations are carried out with various values of physiological parameters to examine the effects of flow parameters on the disturbed flow patterns downstream of a curved artery with a stenosis at the inner wall. The numerical results indicate a strong dependence of flow pattern on the blood viscosity and inlet flow rate, while the influence of the inlet flow profile to the flow pattern in downstream is negligible.

AMS subject classifications: 76D05, 92C50, 76M10

Key words: Curved artery, atherosclerosis, blood flow, wall shear stress, flow pattern.

Dedicated to Professor Yucheng Su on the Occasion of His 80th Birthday

1. Introduction

Atherosclerosis is a disease of large- and medium-size arteries. It preferably develops and progresses at arterial branches, curved artery segments, and artery bifurcations, where the curvature could cause flow irregularity, such as flow shift, flow recirculation, secondary flow, oscillating wall shear stress and fluctuating blood pressure.

Extensive experimental and computational investigations have been made to study the blood flows in arteries with bends or bifurcations and to establish the correlation between the development of the disease and the local haemodynamics [1–11]. Friedman et al. [1] and Nerem et al. [2] have performed experiments that showed an accelerated occurrence of atherosclerosis in human subjects with a coronary geometry. Smedby [3] did an angiographic study in the femoral artery on the direction of growth of plaques, participated by 237 patients with slight or moderate atherosclerosis. Myers et al. [5] investigated the effects of flow waveform and inlet velocity profile on the flow patterns in a model based on the images of a human right coronary artery exhibiting minimal atherosclerotic lesions. Johnston et al. [7] compared models of Newtonian and Non-Newtonian flow in healthy

*Corresponding author. *Email address:* bliu@monmouth.edu (B. Liu)

right coronary arteries with no sign of atheroma. Gach et al. [8] presented a characteristic relationship between the reattachment length in the downstream of a stenosis and the stenotic Reynolds number using MRI. Talukder et al. [9] experimentally studied the effects of the number of stenosis and the distance between consecutive stenoses on the total pressure drop across a series of stenoses. Dash et al. [10] investigated the effect of catheterization on flow characteristics in a curved artery with an axisymmetric stenosis for steady flow with values of Reynolds number up to 100. Nosovitsky et al. [11] studied the flow in a coronary artery model of several degrees of stenosis-like obstruction, where the artery was narrowed around the bend from all surfaces with higher degree of stenosis. Their results showed that coronary artery curvature has an important impact on the intraluminal flow and shear stress. As a result, much has been learned about the haemodynamics in curved arteries.

Although the blood flows in curved arteries have been intensively studied in the past decades, not much work has been reported on the blood flow in single-curved arteries with severe stenosis at the inner wall. The author [12–15] has previously carried out computer simulations of blood flows in curved stenotic arteries and studied the effects of the geometry of the artery, such as the angle of the bend and the size of the stenosis, on the flow patterns. The author also examined the effect of the boundary condition at the artificial outlet boundary on the blood flow in [16] and investigated the difference in the correlations of the flow shift and the blood pressure drop to the change of the Reynolds number by varying the blood viscosity or by varying the mean inlet flow rate [17].

The aim of the present work is to investigate the dependence of the flow patterns downstream of a curved stenotic artery on the flow parameters, such as blood viscosity, inlet flow rate and inlet velocity profile. Emphasis is placed on finding how the wall shear stress and the secondary flow depend on those parameters. Numerical computations are carried out under a variety of physiological flow conditions to investigate the local flow in curved arteries with a stenosis at the inner wall of the bend.

2. Mathematical model

This study assumes that the fluid is laminar, Newtonian, viscous and incompressible and the artery wall is rigid. These assumptions have been shown to be adequate for pulsatile blood flow simulation in artery models under physiological flow conditions by many investigators [7, 18–20]. The time dependent three dimensional Navier Stokes equations are used as the governing equations:

$$\rho(\partial \mathbf{u})/(\partial t) - \nabla \cdot [-p\mathbf{I} + \eta(\nabla \mathbf{u} + (\nabla \mathbf{u})^T)] + \rho(\mathbf{u} \cdot \nabla)\mathbf{u} = 0, \quad \text{in } \Omega, \quad (2.1)$$

$$\nabla \cdot \mathbf{u} = 0, \quad \text{in } \Omega, \quad (2.2)$$

where η is the viscosity of the fluid, $\mathbf{u} = (u_1, u_2, u_3)$ is the flow velocity, p is the internal pressure and ρ is the density of the fluid. The computational domain Ω is a segment of a curved artery with a stenosis at the inner wall as shown in Fig. 1(a).

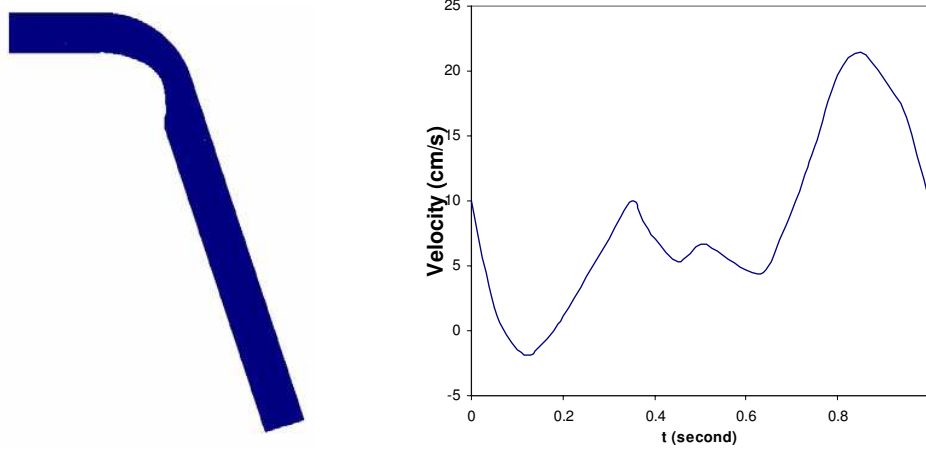


Figure 1: (a) A curved artery with a 72° angle of bend and with a 51% stenosis. (b) Phasic coronary velocity waveform for right coronary artery.

At the inlet boundary, a velocity profile with a pulsatile flow waveform is prescribed:

$$u_1 = U_0 u(r) w(t), \quad u_2 = 0, \quad u_3 = 0, \quad (2.3)$$

where $u(r)$ is a blunt, or a flat, or a parabolic velocity profile with r as the radial distance between a point and the center of the inlet cross section circle; $w(t)$, as shown in Fig. 1(b), is a phasic inflow coronary velocity waveform for the right coronary artery. It is produced by using curve-fitting based on a phasic coronary artery flow velocity curve in Fig. 4 in Matsuo et al. [21], which was recorded in the right coronary artery of a human. It contains a period of reverse flow in systole and a rapid acceleration and deceleration in diastole. U_0 is a scalar chosen as different values in computation such that $U_0 u(r) w(t)$ yields different mean flow rates when examining the effect of the Reynolds number.

The no-slip condition is applied to the velocity at the rigid wall boundary. The outlet boundary is an artificial boundary. The surface traction free boundary condition is imposed at this boundary [5, 22]:

$$(-p\mathbf{I} + \eta(\nabla\mathbf{u} + (\nabla\mathbf{u})^T))\mathbf{n} = 0, \quad (2.4)$$

where $\mathbf{n} = (n_1, n_2, n_3)$ is the outward normal unit vector at the outlet boundary. The initial conditions \mathbf{u}_0 and p_0 are obtained by solving the system of steady state Navier Stokes equations.

3. Parameter setting and numerical method

The computational geometry of the artery has circular cross sections with a 0.45cm diameter at both inlet and outlet and with varying diameters in the region of stenosis. The bend has an angle of 72° with a 0.8cm radius of curvature at the central line of the tube. The neck of the stenosis is at the end of the bend with a reduction of 51% in cross-section area. The straight inlet and outlet tubes are 1.0cm and 4.0cm long, respectively.

The density of the fluid ρ is chosen as 1.05g/cm^3 . When examining the effect of the blood viscosity, η is chosen as 0.0245, 0.0314, and 0.0439 dyne/cm², respectively, while the scalar U_0 for the inlet flow rate is fixed as 1.30. It results in the Reynolds numbers $Re = 453, 353$ and 253, respectively. On the other hand, when examining the effect of the inlet flow rate, the scalar U_0 is chosen as 1.30, 1.01 and 0.73, while η is fixed as 0.0245 dyne/cm². It also results in $Re = 453, 353$ and 253, respectively. When examining the effect of the inlet velocity profile, the scalar U_0 is chosen as 1.22 for flat, 1.30 for blunt, and 2.19 for parabolic inlet velocity profiles, respectively. It results in the same mean reference Reynolds number at the inlet as 453 when η is fixed as 0.0245 dyne/cm².

Navier-Stokes equations are solved using the finite element method with piecewise quadratic functions for velocity and piecewise linear functions for pressure over a tetrahedral mesh. GMRES method with restarting is used to solve the resulted linear system of equations iteratively. Numerical computations are performed using Comsol Multiphysics. Computations are repeated over different meshes to ensure that the numerical solutions are meshing independent. Five cycles are simulated to ensure that the flow is truly periodic.

4. Observations and discussion

Simulations are carried out with various values of physiological parameters to investigate the influences of factors, such as Reynolds number, blood viscosity, inlet flow rate, and inlet velocity profile, on the flow patterns downstream of curved atherosclerotic arteries, including flow shifting, secondary flow, WSS level and pressure drop. In Fig. 2 through Fig. 6, the horizontal axis is the normalized axial length of the artery. $x = 0$ and $x = 1$ correspond to the inlet and outlet boundary, respectively. The straight inlet tube is between $x = 0$ and $x = 0.16$. The curved part is between $x = 0.16$ to $x = 0.33$. The throat of the stenosis is at $x = 0.33$ and the end of the stenosis is at $x = 0.39$.

Influence of the Reynolds number

The Reynolds number is calculated by $Re = \bar{U}d\rho/\eta$, where \bar{U} is the mean inlet velocity at the peak time, d is the diameter of the inlet tube. It is well known that the Reynolds number has a significant effect on the blood flow in stenotic arteries, especially on the flow downstream of the stenosis. Both experimental and mathematical researches on haemodynamics in stenotic arteries have been reported to investigate the influence of the Reynolds number [8, 9, 23]. However, most of these studies were focused on the variation of the Reynolds number due to the change of the flow rate. Not much attention has been paid to the influence of the Reynolds number on the flow characteristics corresponding to the variation of the blood viscosity. The kinematic viscosity of blood can vary between 0.016 and 0.096 cm²/s [24]. A decrease in the blood viscosity will result in an increase in the Reynolds number. Therefore it is also very important to understand the influence of the blood viscosity, in addition to the influence of the flow rate, on the stenotic blood flow when investigating the effect of the Reynolds number.

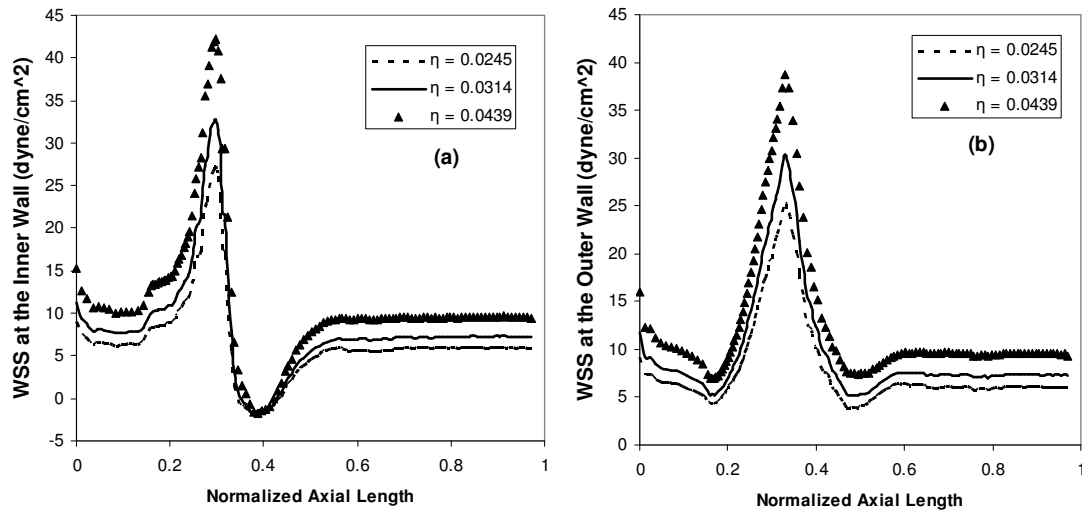


Figure 2: Wall shear stress of the blood flow in curved coronary arteries with different blood viscosities (a) along the inner wall; (b) along the outer wall , at systolic peak ($t = 0.35s$) with a blunt inlet velocity profile.

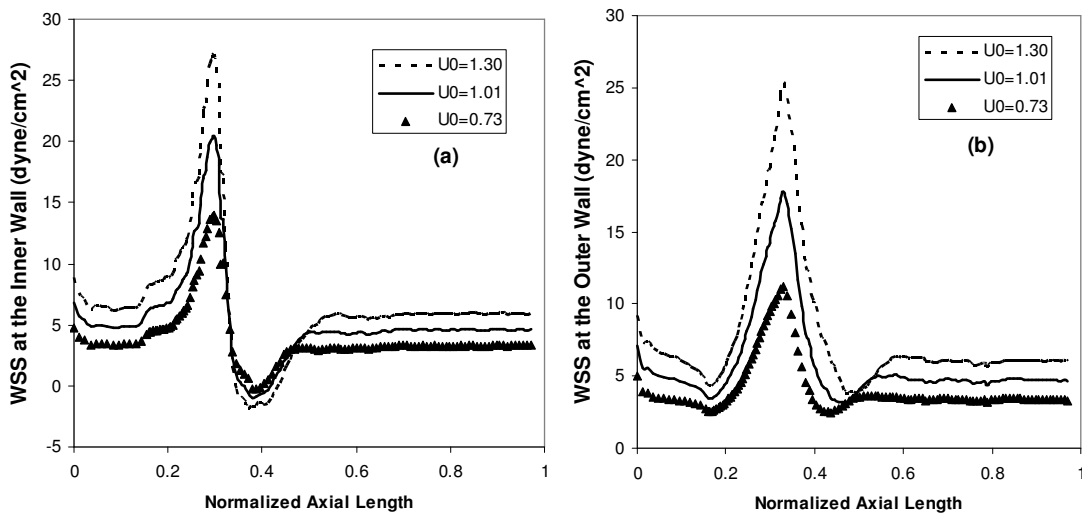


Figure 3: Wall shear stress of the blood flow in curved coronary arteries with different flow rates (a) along the inner wall; (b) along the outer wall , at systolic peak ($t = 0.35s$) with a blunt inlet velocity profile.

The author previously [17] studied the influence of the Reynolds number on the flow patterns in a stenotic coronary artery. Computations were carried out under physiological flow conditions to examine how the characteristics of the flow, such as the maximum flow shift and the pressure drop along the inner wall, change corresponding to the variation of the blood viscosity or to the variation of the mean inlet flow rate. It was observed that some flow characteristics, such as the maximum flow shift, area of flow separation, magnitude of the reverse flow, and the dimensionless pressure drop, correlate to the change of the

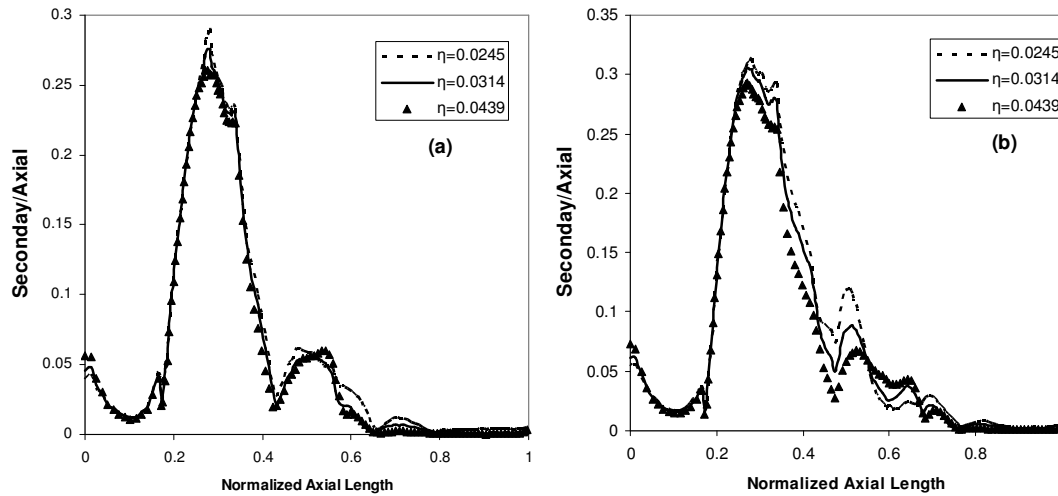


Figure 4: Ratio of the maximum secondary flow to the maximum axial flow of the cross section, effect of viscosity, (a) $t = 0.35s$, (b) $t = 0.4s$, with a blunt inlet velocity profile.

Reynolds number in a similar manner. For instance, as the Reynolds number increases, the maximum flow shifts further towards the outer wall, the dimensionless pressure drop decreases, and the reverse flow at the inner wall is stronger, regardless whether the increase of the Reynolds number is due to the change of the blood viscosity or the inlet flow rate. However, it was also observed in [17] that the response of the axial velocity on the change of the Reynolds number is more sensitive to the variation of the inlet flow rate while that of the dimensionless pressure drop is more sensitive to the blood viscosity.

We now examine the difference in the correlation of the wall shear stress (WSS) to the increase of the Reynolds number caused by decreasing the blood viscosity or by increasing the inlet flow rate. Figs. 2 and 3 are plots of the WSS (in dyne/cm^2) along the inner wall (a) and along the outer wall (b), respectively, at the systolic peak ($t = 0.35s$) during the cardiac cycle in a curved artery of 51% stenosis with a blunt inlet velocity profile. Negative wall shear stresses indicate a reverse flow. These figures show the behavior of the WSS along a curved stenotic artery. Along the inner wall, the WSS peaks at the neck of the stenosis and reaches the minimum in the post-stenosis region, and then recovers gradually in downstream until it levels off. This qualitatively agrees with the observations on the wall shear stress of stenotic blood flows in curved arteries with a phasic inflow velocity waveform for the left coronary artery in [11] and with a phasic inflow velocity waveform for the carotid artery in [15].

Figs. 2 and 3 also demonstrate the effects of the blood viscosity and the inlet flow rate on the WSS, respectively. Each figure contains three WSS curves corresponding to stenotic blood flows with three different Reynolds numbers, $Re=453$, 353, and 253, respectively, resulted by either varying blood viscosity (Fig. 2), or varying inlet flow rate (Fig. 3). By comparing Figs. 2 and 3 we can see that the WSS reacts differently as the Reynolds number increases depending on whether the increase is caused by the change of the blood viscosity or the change of inlet flow rate. Fig. 2 shows that at a higher Reynolds number corre-

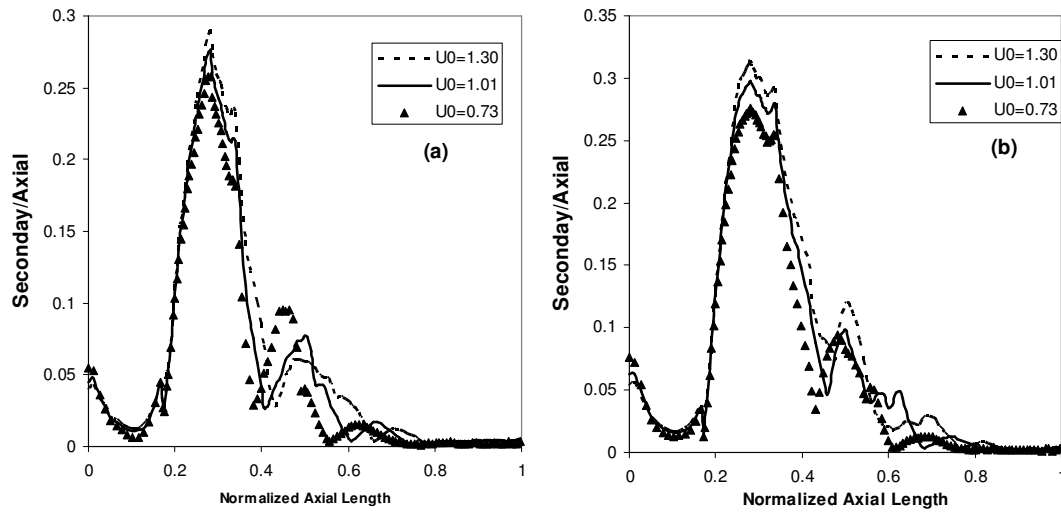


Figure 5: Ratio of the maximum secondary flow to the maximum axial flow of the cross section, effect of flow rate, (a) $t = 0.35s$, (b) $t = 0.4s$, with a blunt inlet velocity profile.

sponding to a smaller viscosity, the overall WSS along both the inner wall and the outer wall is lower. Contrarily, at a higher Reynolds number corresponding to a larger inlet flow rate, the WSS along both the inner wall and the outer wall is higher, except right after the stenosis at the inner wall (Fig. 3).

Secondary flows occur along the curved arteries as a result of acting centrifugal forces. As discussed in [14], the pattern of the secondary flow in a curved stenotic artery is more complex than that in a curved artery with no stenosis. An approach for assessing the secondary flow is to examine the maximum magnitude of the transverse velocity on each cross section. The transverse velocity contains the velocity components perpendicular to the axial velocity. Figs. 4 and 5 plot the ratio of the maximum magnitude of the secondary flow to the maximum axial velocity on each cross section from inlet to the outlet when $t = 0.35s$ in (a) and when $t = 0.4s$ in (b). This ratio reaches a maximum value of around 0.3 at the second half of the curved part in each plot. It indicates that the secondary flow is relatively stronger at the second half of the curved part which is on the order of 30% to the axial velocity. Fig. 4 shows the effect of the blood viscosity and Fig. 5 shows the effect of the flow rate on the secondary flow, respectively. In each case, the Reynolds number changes from 253 to 453 as the blood viscosity decreases from 0.0439 to 0.0245 dyne/cm², or the scalar adjusting the flow rate increases from 0.73 to 1.30. Both figures demonstrate that the secondary flow is strong in a curved stenotic artery and that the ratio of the maximum secondary flow to the maximum axial velocity increases as the Reynolds number increases, regardless of whether the flow rate increases or blood viscosity decreases. Comparing these plots we can see that the variation of the percentage of the secondary flow to the axial velocity corresponding to the change of the blood viscosity is less sensitive than that to the change of the flow rate. At the systolic peak ($t = 0.35s$), the ratio is almost independent of the viscosity except in the regions in the middle of the curved part and the middle of the downstream.

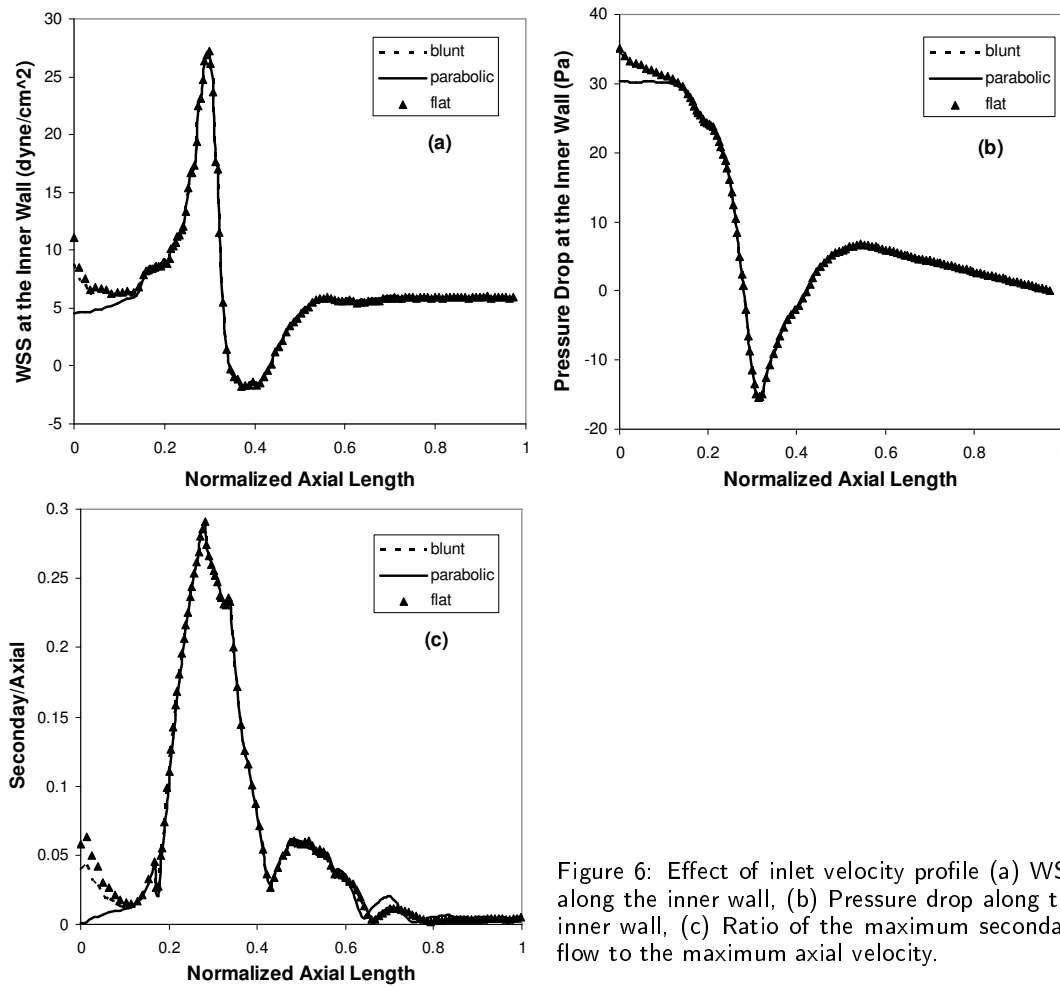


Figure 6: Effect of inlet velocity profile (a) WSS along the inner wall, (b) Pressure drop along the inner wall, (c) Ratio of the maximum secondary flow to the maximum axial velocity.

Influence of the inlet velocity profile

In [5], the effects of the inlet velocity profile and the flow waveform on the flow patterns in a nearly healthy right coronary artery were studied. It was concluded that the changes in the inlet velocity profile did not produce significant change in the arterial velocity and wall shear stress patterns. As we know, the presence of a stenosis in an artery results in major disruption of the normal flow field. The question is whether the changes in the inlet velocity profile will have an impact on the flow patterns in a stenotic coronary artery. Computations are carried out to study the influence of the inlet velocity profile to the blood flow in a curved artery with a moderate stenosis at the inner wall of the artery. Three different inlet velocity profiles are used for $u(r)$ in the boundary condition at the inlet. The first is a blunt velocity profile; the second is a fully developed parabolic velocity profile; and the third is a flat velocity profile. In each case the scalar U_0 is adjusted such that all three cases will result in the same flow rate, so the Reynolds numbers are also the same as 453 with a choice of viscosity 0.0245 dyne/cm^2 .

Fig. 6 shows the effect of the inlet velocity profile on the blood flow in a curved stenotic artery. It has the plots of the WSS along the inner wall (a), pressure drop along the inner wall (b), and the ratio of the maximum secondary flow to the maximum axial velocity of each cross section perpendicular to the axis of the artery (c), at the systolic peak ($t = 0.35s$). In Fig. 6(b) the pressure drop is calculated by $p - p_e$ along the inner wall in the plane of curvature when $t = 0.35s$. Here p_e is a reference pressure selected as the pressure at the outlet. From Fig. 6 we can see that the changes in the inlet velocity profile have no notable effect on the WSS and the pressure drop along the inner wall and the secondary flow pattern of the blood flow in the curved part and in downstream of the artery, even with the presence of a moderate stenosis (51% of cross section area reduction). Along the straight inlet tube of the artery, the flow patterns associated with the blunt and the flat inlet velocity profiles are essentially the same, while that associated with the parabolic inlet velocity profile is different. This is because either blunt or flat flow is gradually developed into a fully developed flow as it moves along the straight inlet tube, while near the entrance the blunt and flat flows have sharper velocity gradients near the wall than the parabolic flow.

Computations are also carried out to compare the effect of the boundary condition at the artificial outlet boundary downstream of curved stenotic arteries. Three commonly used outlet boundary conditions are applied to the model. They are so-called, Neutral condition (surface traction free), Normal Flow/Pressure condition (the normal component of the total force on the boundary is a pressure force), and Outflow/pressure condition (the total force on the boundary is a pressure force). The comparison shows that the impact of the outlet boundary condition on the flow characteristics in the region of interest is negligible as long as the artificial outlet boundary is chosen far enough downstream. This is similar to the observations obtained in [16] for a phasic inflow carotid velocity artery.

In summary, computer simulations are performed to examine the effects of some flow parameters on the flow patterns in a simplified model of a segment of diseased right coronary arteries. Comparison of the numerical solutions demonstrates that the Reynolds number has a significant influence on the wall shear stress. However, it would be ambiguous to simply claim that the wall shear stress changes as the Reynolds number increases since the wall shear stress would change differently corresponding to the increase of the Reynolds number, depending on whether the change is due to the increase of the flow rate or the decrease of the blood viscosity. The percentage of the maximum secondary flow relative to the maximum axial velocity in a curved stenotic artery also increases as the Reynolds number increases, regardless of whether the change in the Reynolds number is resulted from the increase of the flow rate or the decrease of the viscosity. On the other hand, the influence of the different velocity profiles of the inlet boundary condition on the flow patterns downstream of a curved artery with a stenosis at the inner wall is negligible.

Acknowledgments This paper is dedicated to Professor Yucheng Su's 80th birthday. This research was supported, in part, by the Grants-in-Aid for Creativity of Monmouth University.

References

- [1] Friedman M.H., Hutchins G.M., Bargeron C. B., Deters O. J., and Mark FF. Correlation between intimal thickness and fluid shear in human arteries, *Atherosclerosis* , 1981, 39: 425-436.
- [2] Nerem RM, Levesque MJ. The case for fluid dynamics as a localizing factor in atherogenesis. In: 'Fluid Dynamics as a Localizing Factor for Atherosclerosis'. Editors: Schettler G, Nerem RM, Schmid-Schonbein H, Mori H, Diehm C. Springer-Verlag, Heidelberg, 1983; 26-37.
- [3] Smedby O. Do plaques grow upstream or downstream?: An Angiographic study in the femoral artery. *Arterioscler Thromb Vasc Biol.*, 1997, 17: 912-918.
- [4] Gibson CM, Diaz L, Kandarpa K, Sacks FM, et al. Relation of vessel wall shear stress to atherosclerosis progression in human coronary arteries. *Arteriosclerosis and Thrombosis*, 1993, 13: 310-315.
- [5] Myers JG, Moore JA, Ojha M, Johnston KW, Ethier CR. Factors influencing blood flow patterns in the human right coronary artery. *Ann Biomed Eng.*, 2001, 29: 109-120.
- [6] Prosi M, Perktold K, Ding Z, Friedman MH. Influence of curvature dynamics on pulsatile coronary artery flow in a realistic bifurcation model. *J Biomech.*, 2004, 37: 1767-1775.
- [7] Johnston BM, Johnston PR, Corney S, Kilpatrick D. Non-Newtonian blood flow in human right coronary arteries: Transient simulations. *J Biomech.*, 2005, 39: 1116-1128.
- [8] Gach H. M., Lowe I. J. Measuring Flow Reattachment Lengths Downstream of a Stenosis Using MRI. *J Magnetic Resonance Imaging*, 2000, 12: 939-948.
- [9] Talukder, N., Karayannacos, P. E., Nerem, R. M., and Vasko, J. S. An Experimental Study of the Fluid Dynamics of Multiple Noncritical Stenoses. *Journal of Biomechanical Engineering*, 1977, 99: 74-82.
- [10] Dash R.K, Jayaraman G, Mehta KN. Flow in a catheterized curved artery with stenosis. *J. Biomech.*, 1999, 32: 49-61.
- [11] Nosovitsky VA., Ilegbusi OJ, Jiang J, Stone PH, Feldman CL. Effects of curvature and stenosis-like narrowing on wall shear stress in a coronary artery model with phasic flow. *Computers and Biomedical Research*, 1997, 30: 61-82.
- [12] Liu B. Pressure drop in curved atherosclerotic arteries. In: *Advances in Bioengineering*. Editors: Sacks M, Hefzy MS, 2003, BED-Vol. 55: 55-56.
- [13] Liu B. Flow patterns in curved atherosclerotic arteries. *Far East Journal of Applied Mathematics*, 2004, 14: 157-177.
- [14] Liu B. Pulsatile flow in a stenosed right coronary artery. *Far East Journal of Applied Mathematics*. 2006, 25(1): 73-84.
- [15] Liu B. The influences of stenosis on the downstream flow pattern in curved arteries. *Medical Engineering & Physics*. 2007, 29(8): 868-876.
- [16] Liu B. Computer simulations of flows in curved tubes with stenosis. in: *Proceedings of Comsol Multiphysics Conference*, Boston, 2005, pp. 33-37.
- [17] Liu B. Effect of the Reynolds number on the flow pattern in a stenosed right coronary artery. ICCES'07, *Advances in Computational & Experimental Engineering and Sciences*, Edited by Z. Han, S. W. Lee, and M. Nakagaki. 2007. pp. 727-732.
- [18] Duncan D. D., Bargeron C. B., Borchardt S. E., The effect of compliance on wall shear in cast of a human aortic bifurcation, *ASME Journal of Biomechanical Engineering*, 1990, 112: 183-188.
- [19] He X., Ku D. N., Pulsatile flow in the human left coronary artery bifurcation: Average conditions, *Transactions of the ASME*, 1996, 118: 74-82.
- [20] Steinman D. A., and Ethier C. R., Numerical modeling of flow in a disensible end-to-side

- anastomosis, BED-vol. 24, Bioengineering Conference, ASME, 1993, 379-382.
- [21] Matsuo S., Tsuruta M., Hayano M., Imamura Y., Eguchi Y., Tokushima T., Tsuji S. Phasic coronary artery flow velocity determined by Doppler flowmeter catheter in aortic stenosis and aortic regurgitation. *The American Journal of Cardiology*, 1988, 62: 917-922.
- [22] Xu X. Y., Collins M. W., *Haemodynamics of Arterial Organs, Comparison of Computational Predictions with In vitro and In Vivo Data*, WIT Press, 1999, pp. 49.
- [23] Back, L. H., Cho, Y. I., Crawford, D. W. and Cuffel, R. F. Effect of Mild Atherosclerosis on Flow Resistance in a Coronary Artery Casting of Man. *Journal of Biomechanical Engineering*, 1984, 106: 48-53.
- [24] McDonald DA, *Blood flow in arteries*. Baltimore, Williams & Wilkins, 1974.